Matrix pencil method-based reference current generation for shunt active power filters

Terriche, Yacine; Golestan, Saeed; Guerrero, Josep M.; Kerdoune, Djallel; Quintero, Juan Carlos Vasquez

Published in:
IET Power Electronics

DOI (link to publication from Publisher):
10.1049/iet-pel.2017.0351

Publication date:
2018

Document Version
Early version, also known as pre-print

Matrix Pencil Method-Based Reference Current Generation for Shunt Active Power Filters

Yacine Terriche [1*], Saeed Golestan [1], Josep M. Guerrero [1], Djallel Kerdoune [2] Juan C. Vasquez [1]

[1] Department of Energy Technology, Aalborg University, Aalborg East 9220, Denmark
[*] yassine.terriche@yahoo.fr
[2] Department of Electrical Engineering, university of Frères Mentouri Constantine 1, route Ain El Bey 25017, Constantine, Algeria.

Abstract: In recent years, the shunt active power filters (SAPFs) have received much attention for compensating the harmonic pollution and also providing the reactive content. A crucial issue in controlling the SAPF is generating the reference compensating current (RCC). Typical approaches for this purpose are using the discrete Fourier transform (DFT) in the frequency domain, or the instantaneous p-q theory and the synchronous reference frame (SRF) in the time domain. The DFT, however, suffers from the picket-fence effect and spectral leakage. On the other hand, the DFT takes at least one cycle of the nominal frequency. The time domain methods show a weakness under voltage distortion, which require prior filtering techniques. The aim of this paper is to present a fast yet effective method for generating the RCC for SAPFs. The proposed method, which is based on the matrix pencil method (MPM), has a fast dynamic response and works well under distorted and unbalanced voltage. Moreover, the proposed method can estimate the voltage phase accurately, this property enables the algorithm to compensate for both power factor (PF) and current unbalance. The effectiveness of the proposed method is verified using simulation and experimental results, and compared with the standard methods.

1. Introduction

The large spread of electronic equipment based on semi-conductors for AC/DC and AC/AC power conversion has an adverse effect on the power quality. This pollution is well known as harmonics perturbation, which causes harmful effects to both power generation and power transmission [1]-[3]. Traditionally, the mitigation of harmonics and the compensation of the power factor (PF) were attained by using passive power filters (PPFs) [4], because of their simplicity and low cost. These filters, however, suffer from some serious drawbacks such as poor dynamic behaviour, susceptibility to resonance with the load/line impedance, and high sensitivity to the variation in the system parameters. To deal with these problems of the PPFs, the shunt active power filters (SAPFs) have received much attention in recent years [5]. The SAPFs, which are often implemented using voltage source converters, are responsible for generating the total harmonic/reactive content required by the loads. In this way, only the active current required by the loads is drawn from the power system [6], [7].

A critical part in the control of SAPFs is generating the RCC. Indeed, the dynamic behaviour and the accuracy of the SAPF highly depends on the performance of this part. Probably, the most widely used frequency-domain approach for generating the RCC is employing the DFT [8], [9], or the fast Fourier transform (FFT), which is a developed version of the DFT with a collection of algorithms to reduce its computational time [10]-[13]. Nevertheless, the FFT consumes extra power since all frequency bins have to be calculated during the process [14]. Moreover, the FFT provides insufficient performance in analysing a noise-contaminated data [15]-[17]. Besides, the picket-fence effect and spectral leakage disturb the preciseness of the estimated parameters, as well as the complexity in analysing the inter-harmonics [17], [18]. In [12], an online discrete wavelet transform in combination with a least squares algorithm for generating the RCC is proposed. This method is based on down-sampling and decomposing signal into some low- and high-frequency components using a multistage low-pass/high-pass filter and reconstructing the fundamental component using obtained information. This technique, however, cannot extract every single harmonic, which implies it cannot be used in applications where a selective harmonic compensation is demanded. On the other hand, it is a bit difficult to choose the appropriate number of decompositions/stages in the multistage filter and the suitable type of mother wavelet. In the time domain, the P-Q theory and the SRF approach are the most popular methods [19]-[22]. They both offer less computation, and in the existence of the harmonics $6h\pm1$ (h is the harmonic order) they offer a faster transient response compared to frequency domain methods. Moreover, they can effectively compensate for the PF and correct the unbalance. For both techniques, the overall harmonic compensation (OHC) can be implemented. The principle is to use high-pass filters (HPFs) to eliminate the dc component in the d-q frame, which is corresponding to the fundamental component in the stationary frame [23]. While the selective harmonic compensation (SHC) is mainly based on using multiple synchronous reference frame low-pass filters (LPFs) rotating at different angular frequencies for extracting the concerned harmonic frequencies. The rotating angle is provided by a phase-locked loop (PLL). The performance of both OHC and SHC strategies depends on the employed LPFs/HPFs, which are often simple infinite impulse response (IIR) filters [13], [23]-[25]. Using these filters have some disadvantages, mainly the long-time response, the constraints of the appropriate cut off frequency and the filter order, as well as the trade-off existing between improving the accuracy and reducing the response time. Furthermore, both techniques present insufficient

performance in case of voltage distortion which needs prior filtering techniques.

To enhance the SAPF performance, integrating the MPM into the SRF is presented in this paper. The application of MPM in controlling SAPFs has received a little attention, because the MPM is known to be a computationally demanding algorithm. Here, however, it is explained that how the computational burden can be reduced. Indeed, the main principle of the proposed method is converting the harmonic perturbation into a generalized eigenvalue problem, and applying the MPM based on the singular value decomposition (SVD) to solve it. One of the most effective aspects of MPM is the providing a high accuracy when dealing with noisy contaminated data, which offers an accurate assessment of harmonics. Furthermore, the MPM can extract the dc component of the positive sequence signal, as it can also extract the fundamental and each harmonic of a periodic signal under nominal and off-nominal voltage frequency. These properties enable the algorithm to work efficiently under harmonically contaminated and unbalanced voltage, providing equations to estimate the phase of each extract frequency, which allows the compensation of the PF and unbalance.

The rest of the paper is organized as follows. In Section 2, the concept of MPM and its application to dc and ac distorted signals are discussed. In Section 3, the application of MPM to the SAPF is conducted. In Section 4 and 5, simulation and experimental results are presented. Section 6 concludes this article.

2. Matrix pencil method

The matrix pencil is a polynomial approach related to Prony method (PM), which proved that the obstacle of functions' interpolation can be solved by an approximation of a sum of exponentials [26]. Kumaresan and Tufts inserted the SVD inside PM to enhance its noise immunity [27], [28], then the SVD is extended to be applied in MPM [29], [30] [31], taking advantage of the total least square to improve the performance of the method [31], [32]. The appellation Pencil came from the name Pencil of function that is relevant to PM [33]. In [29], a comparison between the MPM and PM is presented. The results indicate that the MPM offers a faster dynamic response and higher noise immunity than the PM. The difference between PM and MPM is that the MPM is one-step process (direct method) while PM is a two-step process in finding the poles $\mathcal{g}_i$[32],[17]. Recently, the MPM has been developed to be applied in various areas, offering better accuracy with a less computational time [30], [17], [34].

Assume that $y(t)$ is the distorted current signal. In this case, according to the PM, it can be approximated by

$$y(t) \cong \sum_{i=1}^{\mathcal{p}} \mathbb{H}_i \cdot e^{(\Im_i t)} + \eta(t) \tag{1}$$

where $\mathbb{H}_i$: Residues or complex amplitudes of i poles.

$\Im_i = -\alpha_i + j\omega_i$

α_i: Damping factors of poles.

ω_i: Angular frequencies ($\omega_i = 2\pi f_i$).

$\eta(t)$: Noise caused during the measurement.

In the discrete-time domain, the data samples Υ are introduced with the sampling period T_s, so (1) can be expressed as:

$$y(\ell T_s) = \sum_{i=1}^{\mathcal{p}} \mathbb{H}_i \cdot \mathcal{g}_i{}^{\ell}\, \mathfrak{H}(\ell T_s) + \eta(\ell T_s) \tag{2}$$

with: ℓ= 0,1, ….,$\Upsilon -1$, $\mathcal{g}_i = e^{(\Im_i Ts)}$, for the tolerance $\mathcal{p}$ we have i = 1,2,…… $\mathcal{p}$.

In order to perform the MPM, the sized data should be structured in the Hankel matrix form, where each descending skew-diagonal from the right side to the left is constant [35], introducing the parameter L that is well known as the pencil parameter as expressed in (3).

$$[Y] = \begin{bmatrix} y(0) & y(1) & \cdots & y(L) \\ y(1) & y(2) & \cdots & y(L+1) \\ \vdots & \vdots & \ddots & \vdots \\ y(\Upsilon-L-1) & y(\Upsilon-L) & \cdots & y(\Upsilon-1) \end{bmatrix}_{(\Upsilon-L)\times(L+1)} \tag{3}$$

According to [17], [32], [33], [35], the algorithm gives the best performance when L is chosen in the interval of $\frac{\Upsilon}{3} \le L \le \frac{\Upsilon}{2}$. However, in case of a periodic undamped signal, the results proved that L gives the best performance when $L = \frac{\Upsilon}{2}$. Also, when applying the MPM in the SRF method to extract the dc component, which is corresponding to the fundamental component in the stationary reference frame, the algorithm gives best performance when $L = 1$. The smaller the value of L, the lower the computational burden is. It implies that using the MPM in the SRF significantly reduces its computational burden.

The SVD is one of the most important decompositions in the linear algebra. It is widely used in the signal processing and statistical methods to characterize and analyze the behavior and the properties of noisy signals. Inside the decomposition, it displays the frequencies variation in a descending order from the most dominant to the smallest. In addition, it offers the possibility to reduce the data by preserving the fundamental with the essential points. As a result, the noisy signal will be filtered and the computation time will be reduced.

In order to perform the SVD of $[Y]$, the product of the three following matrices must be accomplished [35][36].

$$[Y] = [U][D][V]^T \tag{4}$$

$$[U] = \begin{bmatrix} U(0) & U(1) & \cdots & U(\Upsilon-L-1) \\ U(1) & U(2) & \cdots & U(\Upsilon-L) \\ \vdots & \vdots & \ddots & \vdots \\ U(\Upsilon-L-1) & U(\Upsilon-L) & \cdots & U(2\Upsilon-2L-2) \end{bmatrix}_{(\Upsilon-L)\times(\Upsilon-L)} \tag{5}$$

$$[D] = \begin{bmatrix} \sigma(0) & 0 & 0 & 0 \\ 0 & \sigma(1) & 0 & 0 \\ \vdots & \vdots & \ddots & \vdots \\ 0 & 0 & 0 & \sigma(\Upsilon-1) \end{bmatrix}_{(\Upsilon-L)\times(L+1)} \tag{6}$$

$$[V] = \begin{bmatrix} V(0) & V(1) & \cdots & V(L) \\ V(1) & V(2) & \cdots & V(L+1) \\ \vdots & \vdots & \ddots & \vdots \\ V(L) & V(L+1) & \cdots & V(2L) \end{bmatrix}_{(L+1)\times(L+1)} \tag{7}$$

where T represents the transpose of the matrix, the product of $[U]\cdot[U]^T$ and $[V]\cdot[V]^T$ results in the unitary matrix $[I]$,

$[U]$ is an orthogonal matrix that contains the eigenvectors rows of $[Y]\cdot[Y]^T$ and $[V]$ is an orthogonal matrix that contains the eigenvectors rows of $[Y]^T\cdot[Y]$. The diagonal non-negative singular values of the eigenvalues of the matrix $[U]$ or $[V]$ are ordered in a descending rank from the largest left side to the smallest right side, and located in the central diagonal of the rectangular diagonal matrix $[D]$, they appear as pair values for periodic signals, and impair values for non-periodic signals. The rank of the square roots (real values) of $[D]$ is the most important phenomenon of the SVD which exhibits where the intense variation is happening. For the contaminated data $y(\ell Ts)$, selecting $\mathscr{p}$ with the biggest singular value leads to extracting the fundamental component since it contains the biggest value, and selecting $\mathscr{p}$ with the rest singular values leads to extracting the harmonics. The singularity inside $[D]$ is well-defined by the zeros, and the number of non-zeros identifies the matrix rank. The aim of this hypothesis is to calculate $\mathbb{H}_i$ with the best approximation of $\mathscr{g}_i$ and the appropriate selection of $\mathscr{p}$. Since the application of the OHC needs the extraction of only the fundamental, and applying the SHC needs the extraction of only the predominant harmonics. The SVD can be reduced to extract only the needed eigenvalues and their corresponding eigenvectors that conform to the extracted frequencies. As a consequence, the calculation of the pseudo inverse of the matrix $[Y]'$ is reduced and thus the computation of the algorithm is extensively decreased. In MATLAB, the reduced SVD can be obtained using the function (svds) that is shown in (8). The selection of the desired $\mathscr{p}$ leads to obtain the sub-matrices (9), (10) and (11). After the selection of $\mathscr{p}$, the matrix $[Y]$ cannot be reconstructed due to the unfit sizes of $[U_1]$ and $[V_1]^T$. For this reason, $[V_1]$ is reduced into two sub-matrices (12) and (13):

$$[U_1 D_1 V_1] = \text{svds}\,(Y, \mathscr{p}) \tag{8}$$

$$[U_1] = \begin{bmatrix} U(0) & U(1) & \cdots & U(\mathscr{p}-1) \\ U(1) & U(2) & \cdots & U(\mathscr{p}) \\ \vdots & \vdots & \ddots & \vdots \\ U(Y-L-1) & U(Y-L) & \cdots & U(Y+\mathscr{p}-L-2) \end{bmatrix}_{(Y-L)\times(\mathscr{p})} \tag{9}$$

$$[D_1] = \begin{bmatrix} \sigma(0) & 0 & 0 & 0 \\ 0 & \sigma(1) & 0 & 0 \\ \vdots & \vdots & \ddots & \vdots \\ 0 & 0 & 0 & \sigma(2\mathscr{p}-2) \end{bmatrix}_{(\mathscr{p})\times(\mathscr{p})} \tag{10}$$

$$[V_1] = \begin{bmatrix} V(0) & V(1) & \cdots & V(\mathscr{p}-1) \\ V(1) & V(2) & \cdots & V(\mathscr{p}) \\ \vdots & \vdots & \ddots & \vdots \\ V(L) & V(L+1) & \cdots & V(L+\mathscr{p}-1) \end{bmatrix}_{(L+1)\times(\mathscr{p})} \tag{11}$$

$$[V_{a1}] = \begin{bmatrix} V(0) & V(1) & \cdots & V(\mathscr{p}-1) \\ V(1) & V(2) & \cdots & V(\mathscr{p}) \\ \vdots & \vdots & \ddots & \vdots \\ V(L-1) & V(L) & \cdots & V(L+\mathscr{p}-2) \end{bmatrix}_{(L)\times(\mathscr{p})} \tag{12}$$

$$[V_{b1}] = \begin{bmatrix} V(1) & V(2) & \cdots & V(\mathscr{p}) \\ V(2) & V(3) & \cdots & V(\mathscr{p}+1) \\ \vdots & \vdots & \ddots & \vdots \\ V(L) & V(L+1) & \cdots & V(L+\mathscr{p}-1) \end{bmatrix}_{(L)\times(\mathscr{p})} \tag{13}$$

where $[V_{a1}]$ and $[V_{b1}]$ are, respectively, obtained by deleting the last and the first row of $[V_1]$, then each matrix is used to identify a new composition of $[Y]$ as follows:

$$[Y_a] = [U_1][D_1][V_{a1}]^T \tag{13}$$

$$[Y_b] = [U_1][D_1][V_{b1}]^T \tag{14}$$

Very important to note that all these matrices are reduced to be only rows when applying the MPM inside the SRF to extract the dc component, and thus the computation is largely reduced.

Next the eigenvalues λ problem is solved as $[Y]_a - \lambda[Y]_b$ that is facilitated to $[Y]^+{}_a - \lambda[I]$, introducing the sign (+) as the pseudo inverse of the matrix. The DFT which is based on the correlation technique assumes that the frequency of the extracted signal is known. Therefore, under off-nominal supply frequency, the DFT provides less precision. Adapting the window size of the DFT with a PLL to estimate the new supply frequency, results in slow response under distorted supply voltage. However, solving the eigenvalue problem in the MPM is a key factor for estimating the frequency of the extracted signal under off-nominal supply frequency. This advantage enables the adaption of the window to increase the accuracy of the extracted signal. Once $\mathscr{g}_i$ is attained with the frequency that corresponds to the supply voltage frequency, the residues $\mathbb{H}_i$ are simply extracted by the least square solution.

$$\begin{bmatrix} Y(0) \\ Y(1) \\ \vdots \\ Y(Y-1) \end{bmatrix} = \begin{bmatrix} 1 & 1 & \cdots & 1 \\ \mathscr{g}_1 & \mathscr{g}_2 & \cdots & \mathscr{g}_M \\ \vdots & \vdots & \ddots & \vdots \\ \mathscr{g}_1^{(Y-1)} & \mathscr{g}_2^{(Y-1)} & \cdots & \mathscr{g}_M^{(Y-1)} \end{bmatrix} \begin{bmatrix} \mathbb{H}_1 \\ \mathbb{H}_2 \\ \vdots \\ \mathbb{H}_M \end{bmatrix} \tag{15}$$

Fig. 1 is depicted to show the difference between the DFT and the MPM in extracting the fundamental component and the harmonic magnitudes (the scales of the magnitudes are zoomed to provide a better view of the difference between MPM and DFT) of a periodic distorted signal under a drifted frequency (changes from 50 Hz to 51 Hz). Since the DFT needs prior information about the aimed frequencies, it offers less precision under off nominal grid frequency. Constructing the periodic fundamental signal using the phase and the magnitude information of the DFT results in a deformed waveform, with a misinformation of its frequency $(\frac{1}{T_{s1}})$ as shown in Fig.1, subplot (1). However, based on the eigenvalue problem, the MPM extracts the fundamental and the harmonic components as periodic signals with the frequencies that correspond to the entered contaminated signal frequency$\left(\frac{1}{T_{s2}}\right)$, then the extracted signals are served to the least square algorithm to estimate their exact magnitude and phase. In other words, the MPM does not need prior information about the frequency of the contaminated data when dealing with periodic signals. As a result, the fundamental component and the magnitudes of the harmonic components and their frequencies are accurately estimated even under frequency drift as demonstrated in Fig. 1.

3. Application of MPM for controlling SAPF

Fig. 2(a) depicts a three-phase power network system that contains a power supply (230 V, 50 Hz), an isolation transformer with a turns ration of 1, and three non-linear loads that cause harmonic currents in the power

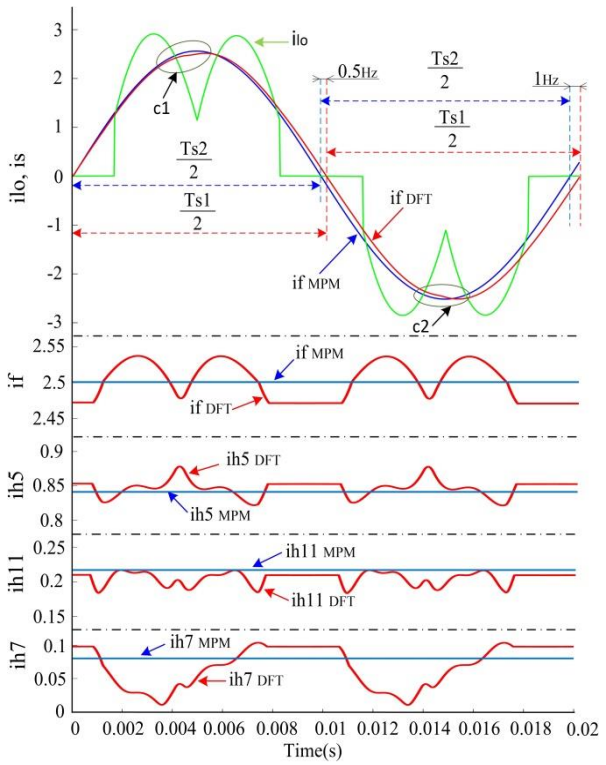

Fig. 1. *Performance of the MPM and the DFT in extracting the periodic fundamental component, and the magnitudes of the fundamental and the 5th, 7th and 11th harmonic components of a distorted signal under frequency variation.*

system, a linear load which affects the PF and cause the unbalance, and a two-level four wires SAPF that is connected to suppress the harmonics and correct both the PF and the unbalance. Fig. 2(b) shows the control structure of the SAPF.

In order to optimize the transient response of the SAPF during the load variation, the SRF-based method is applied. The procedure starts by performing Park's transformation to convert the load currents $i_{lo1,2,3}$ from *abc* system into direct–quadrature–zero (*dqo*) rotating coordinate as expressed in equations (16), (17) and (18):

$$i_d = \frac{2}{3}[i_{lo1}\sin(\phi_1) + i_{lo2}\sin(\phi_2) + i_{lo3}sin(\phi_3)] \quad (16)$$

$$i_q = \frac{2}{3}[i_{lo1}\cos(\phi_1) + i_{lo2}\cos(\phi_2) + i_{lo3}cos(\phi_3)] \quad (17)$$

$$i_0 = \frac{1}{3}[i_{lo1} + i_{lo2} + i_{lo3}] \quad (18)$$

Typically, for separating the dc currents (i_{ddc}, i_{qdc}), which are corresponding to the load fundamental component, and the ac currents (i_{dac}, i_{qac}), which are corresponding to the load harmonic content, ordinary LPFs and the HPFs are used, respectively. However, this technique has some drawbacks such as long time response, constraints of the appropriate cut off frequency and the filter order, as well as low accuracy. The MPM replaces the LPFs and HPFs for providing an accurate extraction of the harmonics using the OHC technique, where the transient response can easily be adapted. The strategy of applying the MPM is achieved by buffering the data of i_d and $i_q$with the number of samples Υ from fast time input to slow time

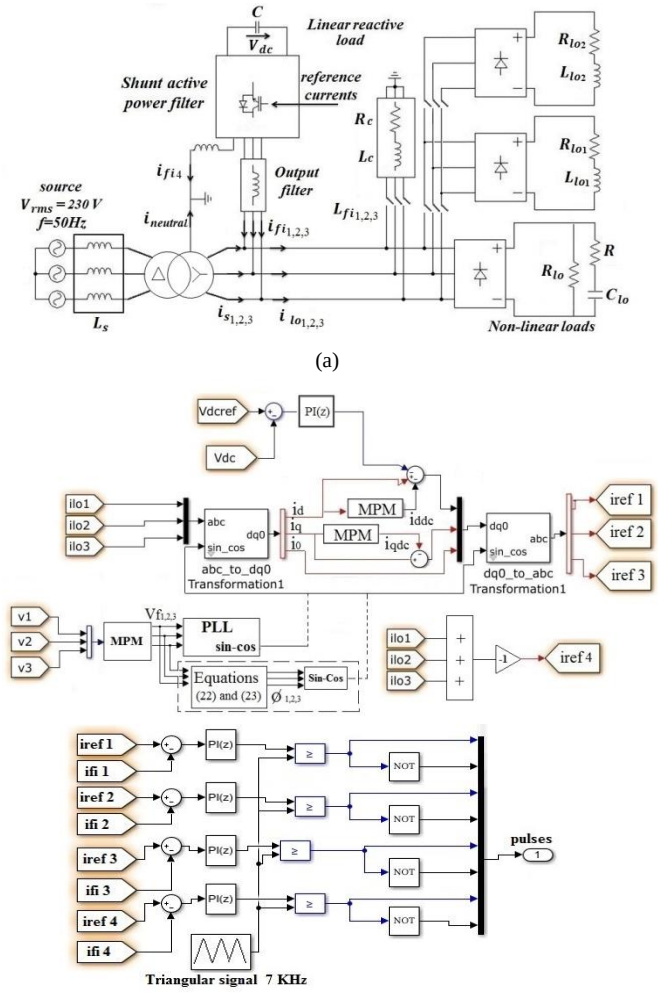

Fig. 2. *Block diagram of SAPF topology*
(a) SAPF schematic diagram, (b) control configuration of the shunt active power filter.

output, then the algorithm of MPM (see section 2) is applied with the selected $\mathcal{p}$. In case of the existence of the harmonics $6h\pm1$, Υ is buffered every $\frac{1}{6}$ cycle (0.0033s) to offer a fast response with an accurate harmonic extraction. In case the unbalance appears, Υ is adapted to be buffered with half cycle (0.01s) when detecting the zero sequence current to give accurate harmonic extraction, and compensate for the unbalance. Next, the extracted continues currents i_{ddc} and i_{qdc} which are corresponding to the load current fundamental component, are reconstructed back from frame based input (slow time) to sample-based output (fast time) using the unbuffer function. To obtain the sum of harmonic currents, i_{ddc} is subtracted from i_d, and i_{qdc} is subtracted from i_q. The DC-link voltage V_{dc} of the SAPF is compared with its reference and added to i_{dac} through a PI controller to compensate for the losses caused by the switches and maintains the DC voltage fixed. After that the inverse Park's is performed to transform from *d-q-0* rotating coordinate into *a-b-c* system as shown below:

$$i_{ref1} = i'_{dac}\sin(\phi_1) + i_q\cos(\phi_1) + i_0 \quad (19)$$

$$i_{ref2} = i'_{dac}\sin(\phi_2) + i_q\cos(\phi_2) + i_0 \quad (20)$$

$$i_{ref3} = i'_{dac}\sin(\phi_3) + i_q\cos(\phi_3) + i_0 \quad (21)$$

The last step is to compare the reference signals $i_{ref1,2,3}$ with the output filter currents $i_{fi1,2,3}$ and send the error to the PWM control through a PI controller. The role of the PI controller is to optimize the dynamic performance of the SAPF by reducing the error and offering a fast response, the comparison is made with a triangular signal of (7 KHz) to create the switches' pulses. The advantage of this control lies in the simplicity and the effectiveness of tracking the references, as well as the controllability of the switches' speed.

In case the voltages $V_{s1,2,3}$ are sinusoidal, the PLL is used to synchronous the reference currents $i_{ref1,2,3}$ with $V_{s1,2,3}$. However, in case $V_{s1,2,3}$ are distorted, the MPM is applied to $V_{s1,2,3}$ in the a-b-c stationary coordinate system to extract the fundamental signals $V_{f1,2,3}$ using the same procedures that are applied to i_d and i_q . The effective performance of the MPM in extracting the fundamentals of $V_{s1,2,3}$ in presence of harmonics enables the use of PLL to give an accurate estimation of the phases $\phi_{1,2,3}$. However, the PLL is a closed loop control system that has a large transient response (probably more than two cycles), and require a high proficiency in designing its controller to avoid instability. The MPM can be considered as an open loop synchronization technique by applying the equations (22) and (23), these equations are developed for MATLAB to estimate $\phi_{1,2,3}$ of $V_{f1,2,3}$ to offer a faster transient response and high stability.

$$[Mag1\ Rank1] = max(u(:)) \tag{22}$$

$$\phi = \left(Rank1 \cdot T_s - \frac{1}{f \cdot 4}\right) \cdot \frac{180}{0.01} \tag{23}$$

where: u(:) is the extracted signal that contains all the samples of the vector, Mag1 and Rank1 are the magnitude and the rank order of the maximum point of $u(:)$, ϕ is the phase.

In the *a-b-c* stationary system, the MPM can extract the harmonics and the fundamental in a half cycle (0.01s) in the presence of the harmonics $6h\pm1$ and the unbalance. According to [17], the MPM can accurately estimate the DC offset. However, since the purpose of applying the MPM to the voltage in this paper is to estimate the phase of the fundamental component, the DC offset can be rejected by applying a derivative to the contaminated data, then the extracted signal is divided by $(2\pi fh)$ (h is the harmonic order of the extracted signal) and its phase is subtracted from $\frac{\pi}{2}$ to cancel the shift and the magnitude augmentation caused by the derivative. In some cases, the derivative can increase the noise, but the MPM is a noise-resilient technique that can work efficiently under noisy contaminated data. The advantage of this technique lies in offering a fast transient response (half cycle in presence of the harmonics $6h\pm1$, unbalance and DC offset) that is not affected by the rejection of the DC offset. Since in this paper the voltage amplitude is considered fixed and the load current is variable, then the rejection of the DC offset can be easily achieved by buffering the data of one cycle and applying equations (24) to the algorithm before equation (2). Equation (24) uses the mean value of the buffered points to extract the DC offset, then (25) rejects the DC offset from the data. It will be demonstrated in Section 4 that this technique is effective even under frequency variations.

$$y_{dc} = \frac{sum(y(\ell T_s))}{\Upsilon} \tag{24}$$

$$y(\ell T_s) = \sum_{i=1}^{\wp} \mathbb{H}_i \cdot \mathcal{g}_i{}^{\ell}\, \mathfrak{H}(\ell T_s) - y_{dc} + \eta(\ell T_s) \tag{25}$$

4. Simulation results

Table 1 displays the parameters used in both simulation and experimental. The simulation studies are conducted under MATLAB/Simulink. The comparison of the MPM, LPF and the DFT is depicted only in subplot 5 in all the simulation figures, and in subplot 4 in the experimental figures to provide enough information about the accuracy and the transient response of the three methods. And the rest subplots are obtained using the MPM.

Fig. 3 is presented to confirm the effectiveness of applying the MPM based on the SRF method to the SAPF. The subplots are respectively displaying: the voltage supply $V_{s1,2,3}$, the distorted load currents $i_{lo1,2,3}$ with a THD of 32%, the improved source currents $i_{s1,2,3}$, the fluctuated direct current i_d, the filtered DC component i_{ddc} using DFT, MPM, and LPF, the inverter output filter currents $i_{fi1,2,3}$ and finally the dc link voltage V_{dc}. The buffering of the signal can be achieved every sample which provide a moving window with a size of 1/6 cycle in case of the harmonics $6h\pm1$, or a half cycle in the appearance of unbalance. But, in order to offer less computation, the signal can be buffered only every 1/6 cycle or every half cycle in

Table I Simulation parameters of the system

Power supply	Voltages RMS values:	$\boldsymbol{V_{s1,2,3}} = 230$ V
	Main impedances:	$\boldsymbol{L_{s1,2,3}} = 0.004\ \boldsymbol{mH}$
		$\boldsymbol{R_{s1,2,3}} = 0.5\ \boldsymbol{\Omega}$
	DC offset:	$\boldsymbol{V_{dcof}} = 40$ V
SAPF	DC-link voltage references	$\boldsymbol{V_{dc}} = 650$-$660$ V
	DC-link capacitor:	C = 2200 $\boldsymbol{\mu F}$
	output filters:	$\boldsymbol{L_{s1,2,3}} = 15\ \boldsymbol{mH}$
		$\boldsymbol{R_{s1,2,3}} = 2.5\ \boldsymbol{\Omega}$
Load	Non-linear load:	$\boldsymbol{R_L} = \boldsymbol{230\Omega}$
		$\boldsymbol{R} = \boldsymbol{57\Omega}$
		$\boldsymbol{C} = 22\ \boldsymbol{\mu F}$
	Connected non-linear loads :	$\boldsymbol{L_{L1}} = 10\ \mathbf{mH}$
		$\boldsymbol{R_{L1}} = \boldsymbol{460\ \Omega}$
		$\boldsymbol{L_{L2}} = 10\ \mathbf{mH}$
		$\boldsymbol{R_{L2}} = 460\ \boldsymbol{\Omega}$
	Linear inductive load:	$\boldsymbol{L_{C\,1,2,3}} = 0.8\ \mathbf{H}$
		$\boldsymbol{R_{C\,1,2,3}} = 54\boldsymbol{\Omega}$
	Linear unbalanced load	$\boldsymbol{R'_{C\,1}} = 230\boldsymbol{\Omega}$
		$\boldsymbol{R'_{C\,1}} = 80\boldsymbol{\Omega}$
		$\boldsymbol{R'_{C\,1}} = 230\boldsymbol{\Omega}$
		$\boldsymbol{R_{L3}} = 100\boldsymbol{\Omega}$
	Linear unbalanced load	$\boldsymbol{L_{L3}} = 0.1\boldsymbol{H}$

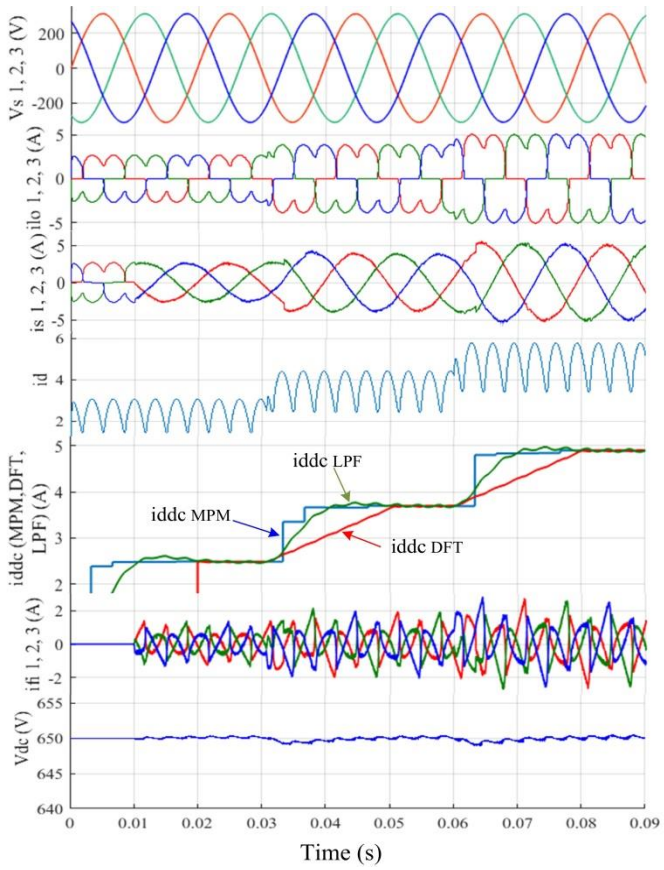

Fig. 3. *Simulation results of harmonic suppression applying MPM.*

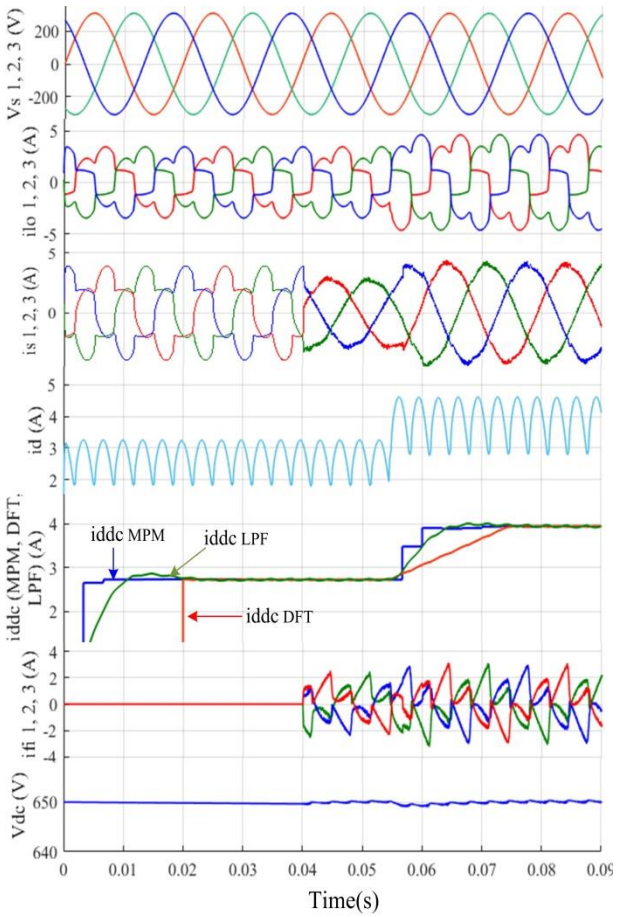

Fig. 4. *Simulation results of harmonic suppression and PF improvement applying MPM.*

the appearance of unbalance. Since the signal is buffered every 1/6 cycle, the response of MPM depends on which instant the variation occurs during buffering the signal. If the variation happens within the first buffered points, the MPM takes 1/6 cycle to estimate the fundamental. If the variation occurs in the other points, then the algorithm gives near information about the fundamental in less than 1/6 cycle. After that, it takes 1/6 cycle to give more precise information as demonstrated in subplot. 5. It is clear that the i_{ddc} extracted by MPM gives accurate information about the fundamental, offering the smallest transient response. In contradiction with the DFT that takes 1 cycle to reach the steady state, and the SRF based on LPF that also show long response with some fluctuations. Applying the MPM to $i_{s1,2,3}$ improves them with the faster response during load variation to reach a THD of less than 3% that respects the IEC 61000-3-6 and IEEE 519-1992 norms.

Fig. 4 demonstrates the capability of the proposed method in suppressing harmonics while compensating the PF. It is obvious that $i_{lo1,2,3}$ are affected by the harmonics with a THD of 28% and the reactive currents that decrease the PF to 0.89%. Connecting the SAPF using the SRF technique based on MPM improves the THD to less than 3%, and compensates for the PF to be near to the unity. Furthermore, it is obvious that i_{ddc} extracted by MPM takes only $\frac{1}{6}$ cycle to give near information about the fundamental in the first period. And in the instant 0.0548s during load variation, it takes less then $\frac{1}{6}$ cycle (0.0019s) to start giving near information about the fundamental, then takes $\frac{1}{6}$ cycle to give precise value. While the DFT and LPF take approximately one period to give information about the fundamental, with some fluctuations caused by the LPF.

Fig.5 presents the behaviour of the proposed method under unbalanced linear and nonlinear variable loads. It is obvious that $i_{lo1,2,3}$ are unbalanced and distorted with a THD of 24% and an unbalance of about 34.6% caused by the linear load. in the instant 0.04s, a single phase nonlinear load is connected to add an unbalance of harmonics. Subplot.3 shows the effect of harmonic distortion and unbalance on i_d. Applying the MPM to the SAPF improves the wave form of $i_{s1,2,3}$ to reach a THD of 1.8% which respects the aformentioned norms. Subplot.5 depicts the response and the accuracy of extracting i_{ddc} using the three abovementioned methods. It is obvious that i_{ddc} extracted by SRF based on MPM is accurate with the smallest response that is changed automaticly to a half period in presence of unbalance, while i_{ddc} extracted by the DFT and the LPF has longer response. Also, the i_{ddc} estimated by LPF causes unaccuracy due to the oscillations introduced by the unbalance. Subplots 6,7,8,9 depict respectively $i_{fi1,2,3}$, the fourth wire current i_{fi4} of the output filter of the inverter that compensates for the unbalance, the compensated neutral current $i_{neutral}$ and V_{dc}. It is clear that when the SAPF is connected in the instance 0.02, $i_{neutral}$ is reduced from around 2.5 A to almost 0.1A.

Fig. 6 proves the efficiency of the proposed method

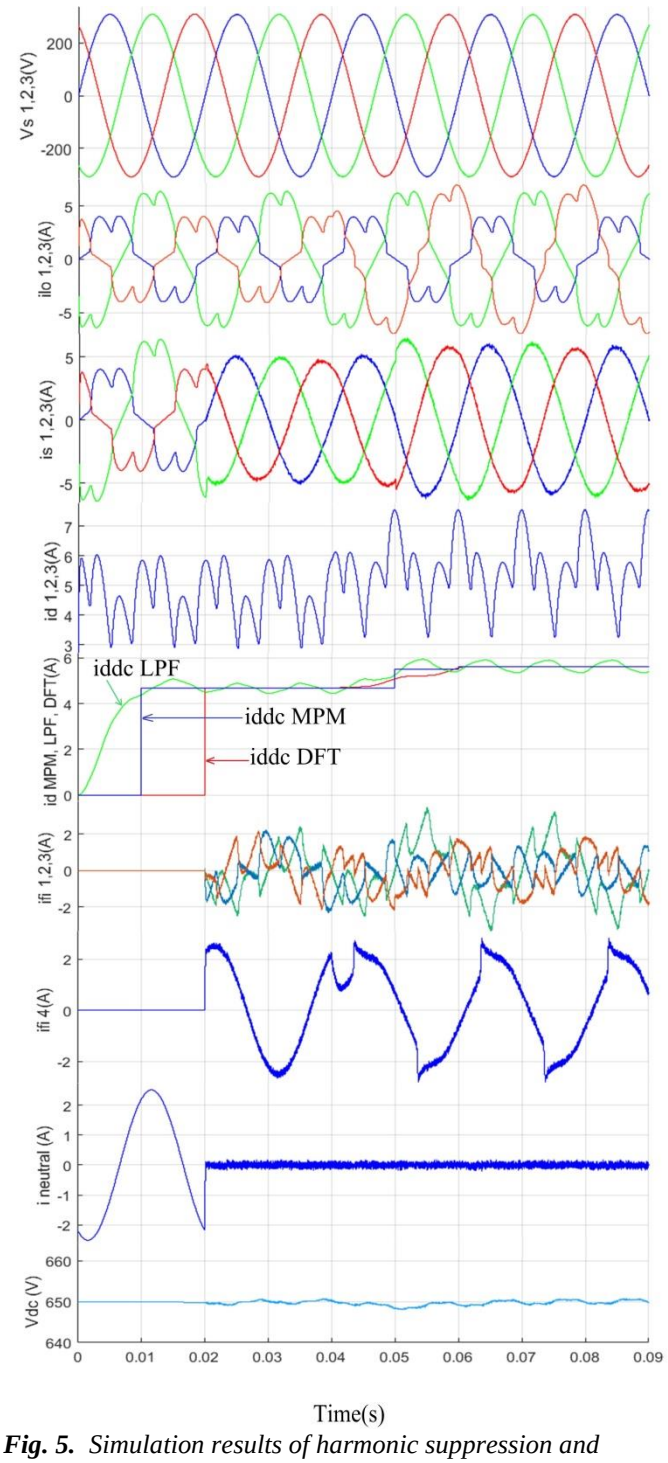

Fig. 5. *Simulation results of harmonic suppression and unbalance compensation applying MPM.*

under voltage distortion. the subplots from 1 to 7 displays $V_{s1,2,3}$ that are Distorted with a THD around 14%. $i_{lo1,2,3}$ that are affected by the harmonics of nonlinear loads and the harmonics of the distorted voltage with a THD of around 28%, $i_{s1,2,3}$ that are improved to a THD of 2.9%, i_d that is affected by load and voltage harmonics, i_{ddc} extracted by the three abovementioed methods, $i_{fi1,2,3}$ that compensate for the source harmonics and finally V_{dc}. $V_{s1,2,3}$ are filtered using MPM, then their phases are extracted using the equations (22) and (23) that are sent to achieve the Park transformation. After that, the MPM is applied to extract i_{ddc} as explained in section III. Applying the MPM to the

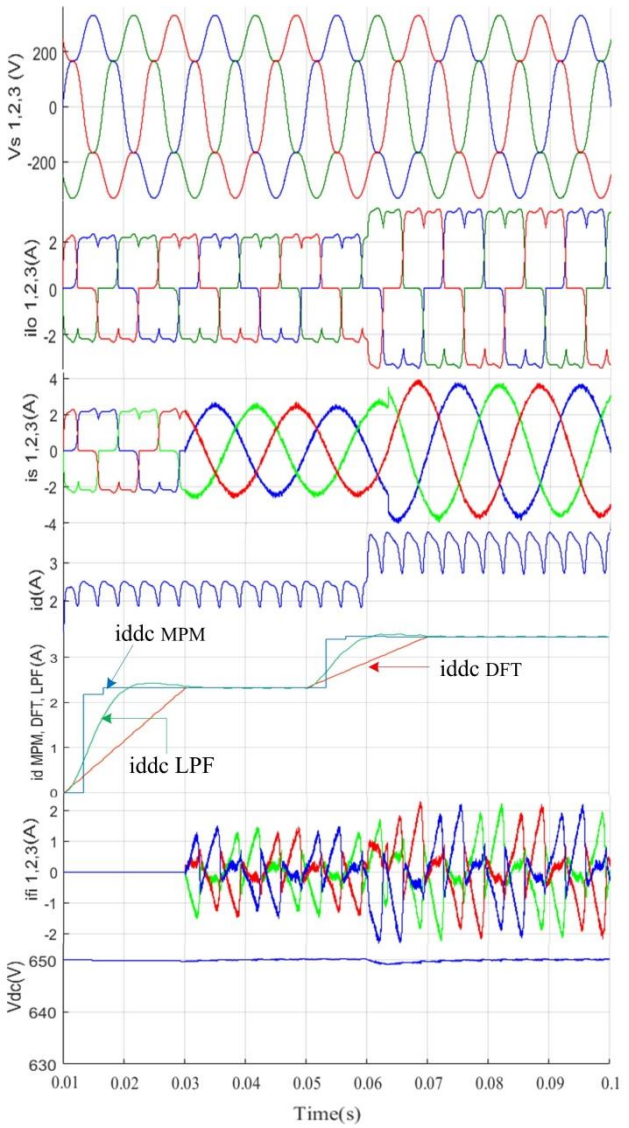

Fig.6. *Simulation results of harmonic suppression under voltage distortion using MPM.*

distorted voltage enables the application of LPF in the d-q-o coordinate to make a comparison. Subplot. 5 shows the response of the three aforementioned methods. It is clear that the MPM provides an accurate extraction with the smallest transient response of $\frac{1}{6}$ cycle during load variation while the other methods cause slow transient response of around one cycle.

Fig. 7 shows the effectiveness of the proposed algorithm under a voltage that is affected by harmonics and dc offset, as well as a drifted frequency (51 Hz). the subplots from 1 to 7 depict respectively: $V_{s1,2,3}$ that are affacted by harmonics with a THD of 14% and a DC offset of 40 V. $i_{lo1,2,3}$ that are harmonically contaminated with a THD of around 28%, $i_{s1,2,3}$ that are improved to a THD of around 4% using the proposed technique, i_d that is affected by load and voltage harmonics, i_{ddc} extracted by the three abovementioed methods, $i_{fi1,2,3}$ that compensate for the source harmonics and V_{dc}. The DC offset of $V_{s1,2,3}$ is rejected using (24) and (25), then the proposed algorithm is applied to extract the phase of the voltage. It is clear that

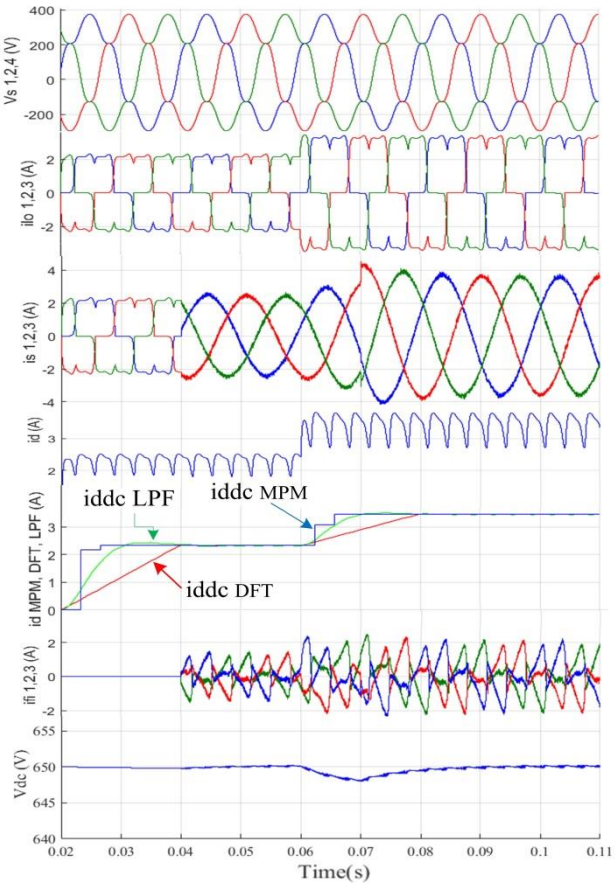

Fig. 7. *Simulation results of harmonic suppression under voltage distortion and dc offset using MPM.*

even under voltage frequency drift and DC offset, the proposed technique offers accurate estimation of the phase, and frequency which enables to perform Park transform and extract the RCC. Since the load is unbalanced and nonlinear, the DC offset of the voltage does not affect the current. However, in case the load current is affected by the DC offset, it can be rejected by expanding the window size of the buffered data of i_d.

5. Experimental results

Fig. 8 depicts the experimental prototype of the SAPF developed in the laboratory. The setup consists of: a three phase isolation transformer with a leakage inductance of 0.8 mH, a digital signal processor (dspace-1006), Hall effect current and voltage sensors, and a Danfoss 2.2 kVA converter with an output L-filter. The THD of the $i_{s1,2,3}$ is measured using the power quality analyzer (Fluke 437). The output filter is situated inside the setup, the sampling time is 10 kHz.

Fig. 9 displays the experimental results that prove the effectiveness of the MPM in harmonic suppression during load variation. $i_{lo1,2,3}$ are distorted with a THD of 32%. The application of park transformation results in the oscillated direct current i_d. It is observable that during the load variation, the i_{ddcs} extracted by DFT and LPF cause slow transient response (almost one period). Moreover, the i_{ddcs} extracted by LPF contain some fluctuations that decrease the accuracy. However, the i_{ddc} extracted by the MPM offers a faster transient response with the higher precision. Consequently, applying the MPM to the SAPF

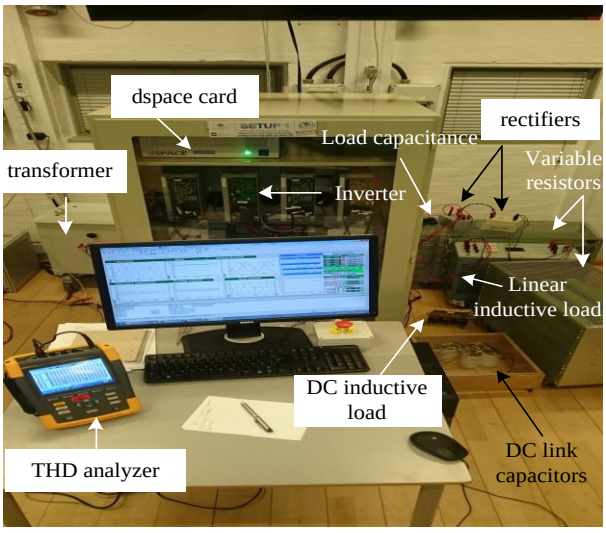

Fig. 8. *Experimental prototype of the SAPF*

results in improving the wave form of $i_{s1,2,3}$ by decreasing the THD to about 4.4% which conforms to the IEC 61000-3-6 and IEEE 519-1992 standards. Furthermore, the transient response of $i_{s1,2,3}$ takes only $\frac{1}{6}$ cycle to be improved.

Fig. 10 shows the experimental results that demonstrate the reliability of the proposed technique in extracting the fundamental during PF compensation. When the load variation occurs in the instant 0.698s, the direct current i_d increases progressively due to the existence of the reactive power. It is clear that the i_{ddc} extracted by the MPM follows the progressive variation faster than the ones

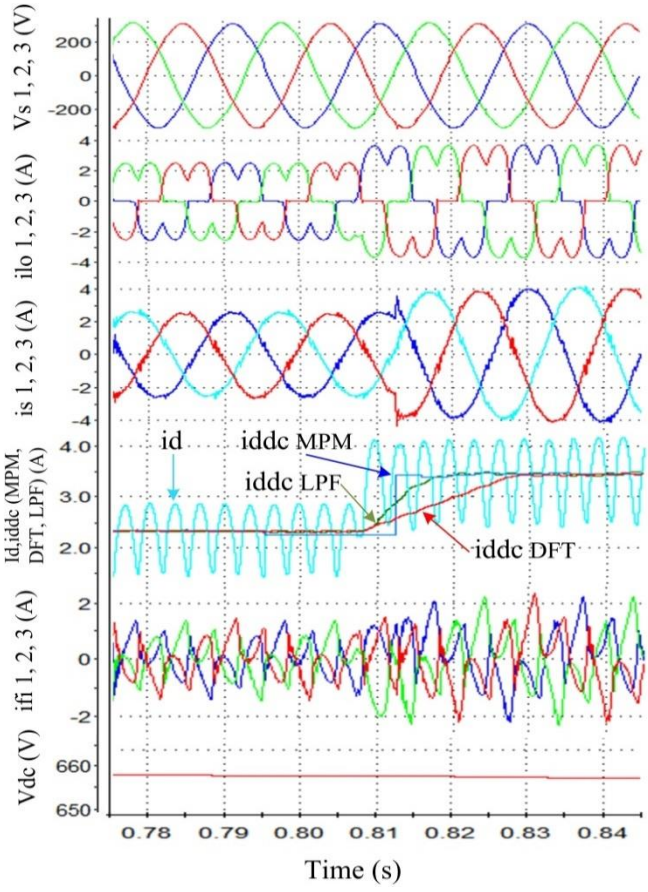

Fig. 9. *Experimental results of harmonic suppression applying MPM.*

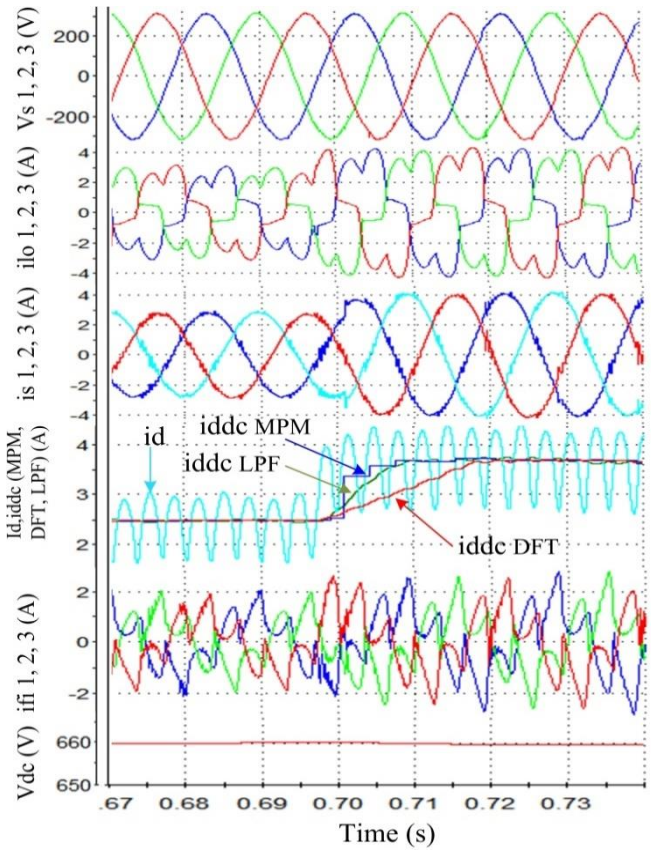

Fig. 10. *Experimental results of harmonic suppression during PF compensation applying MPM.*

extracted by DFT and LPF, and offers more accuracy. As a consequence, the dynamic performance of the SAPF that is based on MPM is improved, which leads to decrease the THD of $i_{s1,2,3}$ from 28% to 4.4% that conforms to the aforementioned standards. Besides, the PF is improved from about 0.9 to be close to unity.

6. Conclusion

In this paper, the MPM based harmonic control strategy for SAPF is proposed. The harmonic perturbation is introduced as an eigenvalue problem, then the MPM is applied to solve it. The proposed method proved its accuracy and efficiency in extracting the desired frequencies in both stationary and rotating coordinates under sinusoidal and distorted voltage. Moreover, the MPM demonstrated its reliability of improving the dynamic performance of the four legs SAPF to compensate for the unbalanced linear and nonlinear loads, offering the faster transient response comparing to standard methods. The simulation of the analyzed model is carried out under MATLAB\Simulink environment, and the results demonstrate the reliability of the proposed method in harmonics assessment, PF and unbalance correction in case of sinusoidal and distorted voltage with harmonics and DC offset. The results are enhanced by the experiment offering a comparison with standards methods.

REFERENCES

[1] Smith, R. L., Stratford, R. P.: 'Power system harmonics effects from adjustable-speed drives', *IEEE Trans. Ind. Appl*., 1984, vol. IA-20, no. 4, pp. 973-977

[2] Ortmeyer, T. H., Chakravarthi, K. R., Mahmoud, A. A.: 'The effects of power system harmonics on power system equipment and loads', *IEEE Power Eng. Rev*., 1985vol. PER-5, no. 9, pp. 54-54.

[3] Rice, D. E.: 'Adjustable speed drive and power rectifier harmonics-Their effect on power systems components'. *IEEE Trans. Ind. Appl*., 1986, vol. IA-22, no. 1, pp. 161-177

[4] Kawann, C., Emanuel, A. E.: 'Passive shunt harmonic filters for low and medium voltage: A cost comparison study', *IEEE Trans. Power Syst*., 1996, vol. 11, no. 4, pp. 1825-1831

[5] Singh, B., Al-Haddad, K., Chandra, A.: 'A review of active filters for power quality improvement', *IEEE Trans. Ind. Electron*., 1999, vol. 46, no. 5, pp. 960-971

[6] Odavic, M., Biagini, V., Sumner, M., Zanchetta, P.: 'Low carrier–fundamental frequency ratio PWM for multilevel active shunt power filters for aerospace applications', *IEEE Trans. Ind. Appl*., 2013, vol. 49, no. 1, pp. 159-167

[7] Chang, G. W.: 'A new approach for optimal shunt active power filter control considering alternative performance indices', *IEEE Trans. Power Del*., 2006, vol. 21, no. 1, pp. 406-413

[8] Sozański, K. P.: 'Harmonic compensation using the sliding DFT algorithm for three-phase active power filter', Electrical Power Quality and Utilisation. Journal 12.2 (2006): 15-20

[9] Borisov, K., & Ginn, H.: 'A novel reference signal generator for active power filters based on Recursive DFT', 2008 Twenty-Third Annual IEEE Applied Power Electronics Conference and Exposition, Austin, TX, 2008, pp. 1920-1925

[10] Jiang, R. M.: 'An area-efficient FFT architecture for OFDM digital video broadcasting', *IEEE Trans. Consum. Electron*., 2007, vol. 53, no. 4, pp. 1322-1326

[11] Hsue, W. L., & Chang, W. C.: 'Real discrete fractional Fourier, Hartley, generalized Fourier and generalized Hartley transforms with many parameters', *IEEE Trans. Circ. Syst—I: Regular Papers*, 2015, vol. 62, NO. 10, pp. 2594-2605

[12] Forghani, M., & Afsharnia, S.: 'Online wavelet transform-based control strategy for UPQC control system', *IEEE Trans. Power Del*., 2007, vol. 22, no. 1, pp. 481-491

[13] Asiminoael, L., Blaabjerg, F., & Hansen, S.: 'Detection is key-Harmonic detection methods for active power filter applications', *IEEE Ind. Appl. Mag*., 2007, vol. 13, no. 4, pp. 22-33

[14] Juan, Y. H., Huang, H. Y., Lai, S. C.: 'A distortion cancellation technique with the recursive DFT method for successive approximation analog-to-digital converters', *IEEE Trans. Circ. Syst, II: Express Briefs*, 2016, vol 63, no 2,pp. 146 – 150

[15] Offelli, C., Petri, D.: 'Weighting effect on the discrete time Fourier transform of noisy signals', *IEEE Trans. Instrum. Meas*., 1991, vol. 40, no. 6, pp. 972–981

[16] Wen, H., Guo, S., Teng, Z.: 'Frequency estimation of distorted and noisy signals in power systems by FFT-based approach', *IEEE Trans. Power Syst*., 2014, vol. 29, no. 2, pp. 765–774

[17] Sheshyekani, K., Fallahi, G., Hamzeh, M., & Kheradmandi, M.: 'A general noise-resilient technique based on the matrix pencil method for the assessment of harmonics and interharmonics in power systems', *IEEE Trans. Power Del*., 2017, vol. 32, no. 5, pp. 2179-2188

[18] Testa, A., et al.: 'Interharmonics: theory and modeling', *IEEE Trans. Power Del*., 2007, vol. 22, no. 4, pp. 2335-2348

[19] Akagi, H., Kanazawa, Y., & Nabae, A.: 'Instantaneous Reactive Power Compensators Comprising Switching Devices without Energy Storage Components', *IEEE Trans. Ind. Appl*., 1984, vol. IA-20, no. 3, pp. 625-630

[20] Ovalle, A., Ramos, G., Bacha, S., Hably, A., & Rumeau, A.: 'Decentralized control of voltage source converters in microgrids based on the application of instantaneous power theory', *IEEE Trans. Ind. Electron.*, 2015, vol. 62, no. 2, pp. 1152-1162

[21] Mattavelli, P.: 'Synchronous-frame harmonic control for high-performance AC power supplies', *IEEE Trans. Ind. Appl*., 2001, vol. 37, no. 3, pp. 864-872

[22] Pigazo, A., Moreno, V. M., & Estebanez, E. J.: 'A recursive park transformation to improve the performance of synchronous reference frame controllers in shunt active power filters', *IEEE Transs. Power Electron.*, 2009, vol. 24, no. 9, pp. 2065-2075

[23] Sergej, K., Asiminoaei, L., & Hansen, S.: 'Harmonic detection methods of active filters for adjustable speed drive applications', 2009 13th European Conference on Power Electronics and Applications, Barcelona, 2009, pp. 1-10

[24] Bhattacharya, S., Frank, T. M., Divan, D. M., & Banerjee, B.: 'Active filter system implementation', *IEEE Ind. Appl. Mag*., 1998, vol. 4, no. 5, pp. 47-63

[25] Asiminoaei, L., Blaabjerg, F., & Hansen, S.: 'Evaluation of harmonic detection methods for active power filter applications', Applied Power Electronics Conference and Exposition, 2005. APEC 2005. Twentieth

Annual IEEE, Vol. 1, pp. 635-641
[26] Prony, R.: 'Essai expérimental et analytique, etc.', Paris J. 1'Ecole polytechnique Floréal et Plairial, 1795, vol 1, cahier 22, pp. 24-76
[27] Kumaresan, R., & Tufts, D.: 'Estimating the parameters of exponentially damped sinusoids and pole-zero modeling in noise', *IEEE Trans. Acoust., Speech, Signal Process*., 1982, vol. 30, no. 6, pp. 833-840
[28] Tufts, D. W., & Kumaresan, R.: 'Estimation of frequencies of multiple sinusoids: Making linear prediction perform like maximum likelihood', *Proceedings of the IEEE*, 1982, vol. 70, no 9, pp. 975-989
[29] Hua, Y., & Sarkar, T. K.: 'Matrix pencil method for estimating parameters of exponentially damped/undamped sinusoids in noise', *IEEE Trans. Acoust., Speech, Signal Process*., 1990, vol. 38, no. 5, pp. 814-824
[30] Gaber, A., & Omar, A.: 'A study of wireless indoor positioning based on joint TDOA and DOA estimation using 2-D matrix pencil algorithms and IEEE 802.11 ac', *IEEE Trans. Wireless Commun*., 2015, vol. 14, no. 5, pp. 2440-2454
[31] Adve, R. S., Sarkar, T. K., Pereira-Filho, O. M., & Rao, S. M.: 'Extrapolation of time-domain responses from three-dimensional conducting objects utilizing the matrix pencil technique', *IEEE Trans. Antennas Propag.*, 1997, vol. 45, no. 1, pp. 147-156
[32] Sarkar, T. K., & Pereira, O.: 'Using the matrix pencil method to estimate the parameters of a sum of complex exponentials', *IEEE Trans. Antennas Propag.*, 1995, vol. 37, no. 1, pp. 48-55
[33] JAIN, V. Filter analysis by use of pencil of functions: Part I. IEEE Trans. Circuits Syst., 1974, vol. 21, no 5, p. 574-579.
[34] Chahine, K., Baltazart, V., & Wang, Y.: 'Parameter estimation of damped power-law phase signals via a recursive and alternately projected matrix pencil method', *IEEE Trans. Antennas Propag*., 2011, vol. 59, no. 4, pp. 1207-1216
[35] Yilmazer, N., Koh, J., & Sarkar, T. K., 'Utilization of a unitary transform for efficient computation in the matrix pencil method to find the direction of arrival', *IEEE Trans. Antennas Propag*., 2006, vol. 54, no. 1, pp. 175-181
[36] Cui, Y., Wei, G., Wang, S., Fan, L., & Zhao, Y.: 'Fast analysis of reverberation chamber using FDTD method and matrix pencil method with new criterion for determining the number of exponentially damped sinusoids', *IEEE Trans. Electromagn. Compat*., 2014, vol. 56, no. 3, pp. 510-519